Supplemental Figure Legends

Figure S1. Viral replication of HIV-1 CA G116A in primary T cells. Primary PBMC used for the viral replication assay were separated from whole blood by the Ficoll-Hypaque method. Purified CD4+ T cells were cultured in RPMI 1640 medium containing 5 μg/ml PHA and 20 IU/ml human recombinant IL2 for 3 days. HIV-1 NL4-3 and NL4-3 CA G116A viruses were generated by transfecting HEK293T cells. Virus stocks were assessed for CAp24 concentration using an HIV-1 p24 ELISA Assay kit (XpressBio, Frederick, MD). Equal amounts of virus were used to infect activated T cells and infected cells were washed 6h after infection. Newly produced virus in the supernatants of infected cultures were determined by (A) CAp24 ELISA and (B) a viral infectivity assay using TZM-bl cells. Results shown are the average of three independent experiments. N.I.; no infection.

Figure S2. The distribution of CA 87 and 207 variants in global HIV-1 group M subtypes A, B, C and D.

Figure S3. A diagram of HIV-1 genome indicating subtype B and subtype C HIV-1 recombination in CRF08. (A) Deduced genomic structure of the full-length HIV-1 CRF08 recombinants detected from Guangxi Province in 1997. CRF08 (97CNGX-6F) from Guangxi was mostly subtype C (Red) with portions of gag (CA, Capsid) and pol (RT, Reverse Transcriptase) genes from subtype B (Purple). (B) Evolution of CA point mutations in CRF08. B, subtype B (Purple); C, subtype C (Red). Amino acid position 116 is shown with a black triangle.

Figure S4. Evolutionary changes of HIV-1 CA position 207 during CRF08 transmission in southern China. The arrows indicate potential HIV-1 transmitting routes in southern China. The pie charts show the proportion of viral CA variants at position 207 during CRF08 transmission in southern China. Red (P207), purple (S207), green (A207) and blue (others).

Figure S5. Evolutionary changes of HIV-1 CA position 208 during CRF08 transmission in southern China. The arrows indicate potential HIV-1 transmitting routes in southern China. The pie charts show the proportion of viral CA variants at position 208 during CRF08 transmission in southern China. Red (G208), purple (A208), and brown (T208).

Figure S6. Association of MxB-resistant CA variants with MxB. HIV-1 Wild type or its mutants H87P, G116A and P207A were used to infect MxB-expressing K562 cells. At 20 hours after infection, cells were harvested and suspended in lysis buffer for 3h at 4°C. Cell lysates were then incubated with the anti-HA agarose (Roche) for 6 hours at 4°C. After washing the agrose, the bound MxB was eluted with HA peptide (Sigma) and the amounts of associated HIV-1 CAp24 were determined by ELISA. (A) Cell lysates were analyzed by immunoblotting with the indicated antibodies. (B) Levels of the eluted MxB-HA were assessed by western blotting. The amount of CAp24 eluted from the agarose was determined by ELISA, then standardized by the CAp24 levels in the corresponding cell lysates. Results are representative of four independent experiments. Each bar is the average of three replicates from the same experiment (error bars indicate standard deviations).

Figure S7. Viral core binding is not the only determinant of MxB antiviral activity. (A) Schematic of MxB constructs. (B) Relative infectivity of HIV-1 in presence or absence of the indicated MxB WT or mutant transduced K562 cells. The infectivity was measured 48h after viral infection using flow cytometry to detect GFP positive cells. (C) HIV-1 core association of the wild type MxB and indicated mutants. HIV-1 viruses were exposed briefly to 0.1% Triton X-100, mixed with soluble MxB containing cell lysates and subsequently loaded onto step sucrose gradients. The individual gradient fractions representing soluble MxB (F1) and core-associated MxB (F3) were subjected to immunoblot analysis. A specific antibody against HIV-1 CAp24 was used to detect HIV-1 core.

Figure S8. Cyclophilin A-binding is critical for MxB anti-HIV-1 activity. (A) HIV-1 capsid mutant G89V confers HIV-1 resistance to MxB. MxB transduced or control K562 cells were challenged with equal titers of HIV-1 GFP or HIV-1 G89V GFP viruses. 48h later, cells were harvested for flow cytometric analysis. (B) Cyclosporin A (CsA) treatment blocks MxB anti-HIV-1 activity. MxB transduced or control K562 cells were infected with HIV-1 GFP viruses in the presence or absence of CsA. Infected cells (GFP positive) were analyzed by flow cytometry.

Figure S9. The sensitivity to MxB by HIV in a Cyclophilin A-binding independent manner. (A) Sequence alignment of the CypA-binding loops of HIV-1, HIV2, and HIV-2 P86HA mutant capsids. (B) The P86HA mutation in HIV-2 leads to CypA incorporation in viral particles. Viral particles were analyzed by immunoblotting using specific antibody against Gag/CA and CypA. (C) Relative infectivity of HIV-1 or HIV-2 viruses in MxB expressing K562 cells or control K562 cells. The infectivity was measured 48h after viral infection by using flow cytometry to detect GFP positive cells.

Figure S10. The antiviral activity of MxB is a cell type-depedent manner. (A) Jurkat cells were pretreated with or without 500 U ml−1 IFN-α. 24h later, cells were challenged by equal amount of HIV-1 NL4-3 viruses. The infectivity was measured 48h after viral infection by using flow cytometry to detect GFP positive cells. Results are representative of four independent experiments. Each bar is the average of three replicates from the same experiment (error bars indicate standard deviations). (B) The expression of endogenous MxB of indicated cells were detected by immune blotting by using the indicated antibodies.

Figure S11. MxB resistant-HIV-1 capsid mutants are located in the raised surface of the HIV-1 capsid hexamer. (*Up*) Location of CA amino acid residues important for HIV-1 evasion of the inhibition of MxB on the structural model of the CA hexamer (PDB: 3GV2). Three CA residues H87, G116, P207 are colored in

blue, pink and red, respectively. (*Down*) The schematic of the capsid hexamer. The locations of the three CA mutants are indicated with discontinuous red line.

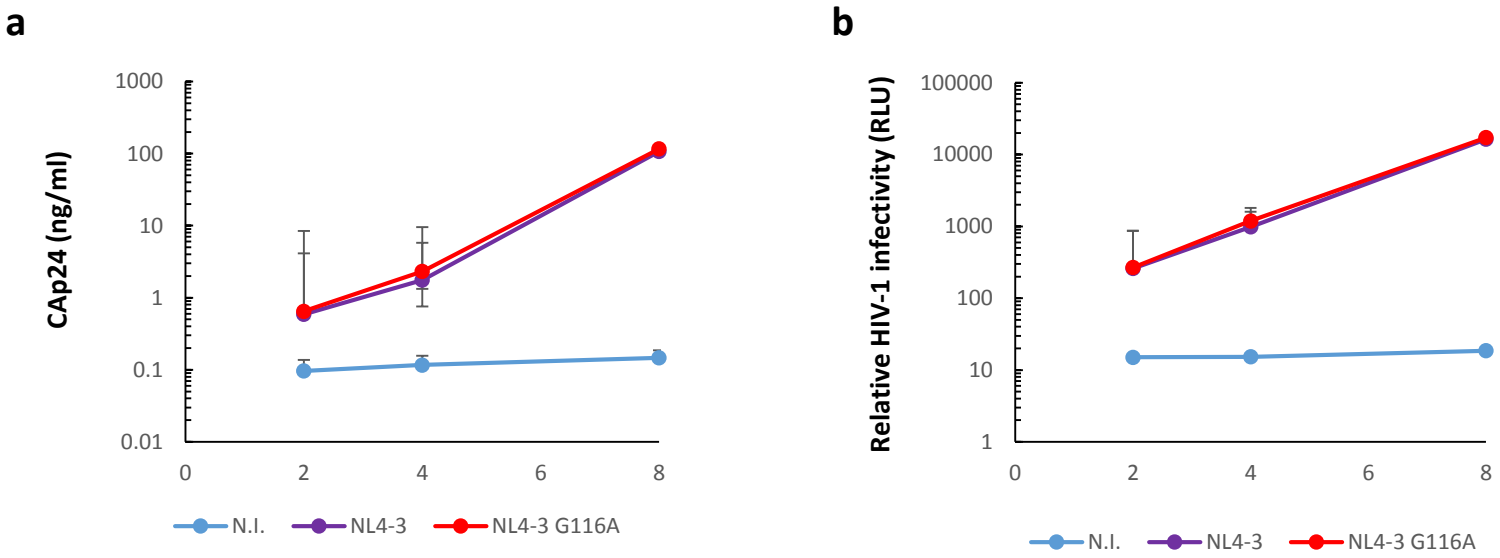
a
CAp24 (ng/ml)
1000
100
10
1
0.1
0.01
0
2
4
6
8
N.I.
NL4-3
NL4-3 G116A
b
Relative HIV-1 infectivity (RLU)
100000
10000
1000
100
10
1
0
2
4
6
8
N.I.
NL4-3
NL4-3 G116A

Fig. S1

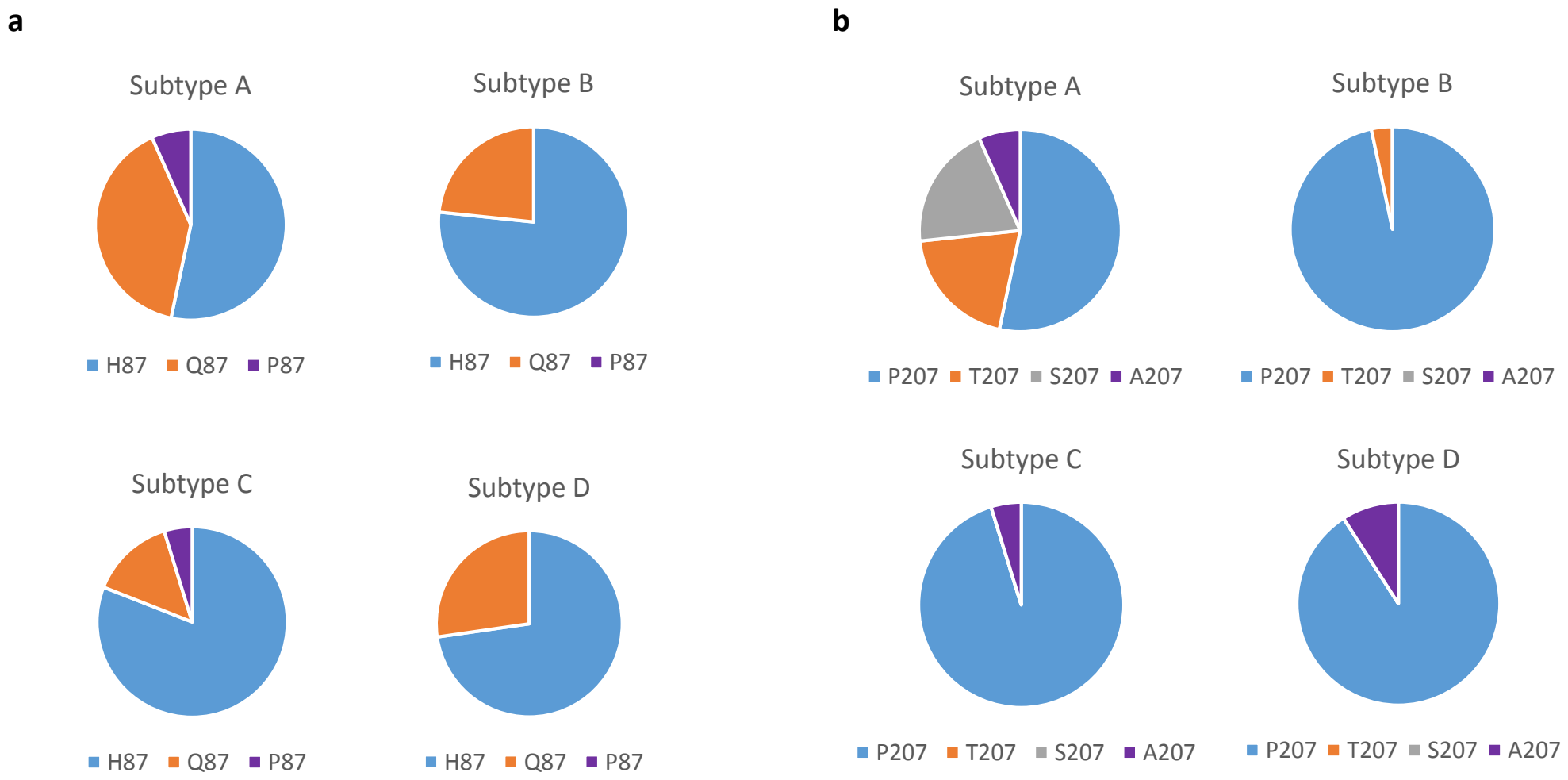
a
Subtype A
H87 Q87 P87
Subtype B
H87 Q87 P87
Subtype C
H87 Q87 P87
Subtype D
H87 Q87 P87
b
Subtype A
P207 T207 S207 A207
Subtype B
P207 T207 S207 A207
Subtype C
P207 T207 S207 A207
Subtype D
P207 T207 S207 A207

Fig. S2

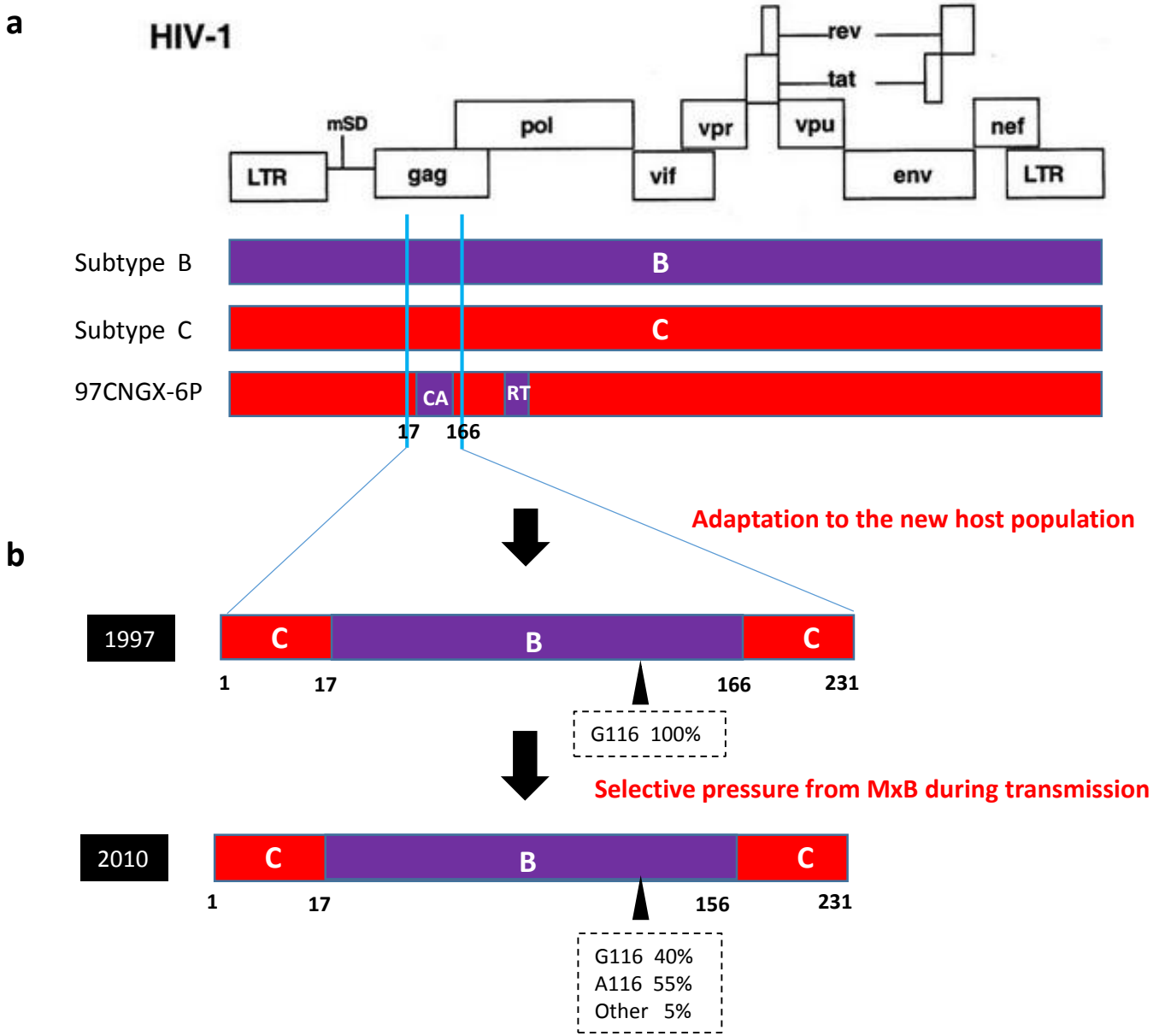
a
HIV-1
rev
tat
mSD
pol
vpr
vpu
nef
LTR
gag
vif
env
LTR
Subtype B
B
Subtype C
C
97CNGX-6P
CA
RT
17
166
Adaptation to the new host population
b
1997
C
B
C
1
17
166
231
G116 100%
Selective pressure from MxB during transmission
2010
C
B
C
1
17
156
231
G116 40%
A116 55%
Other 5%

Fig. S3

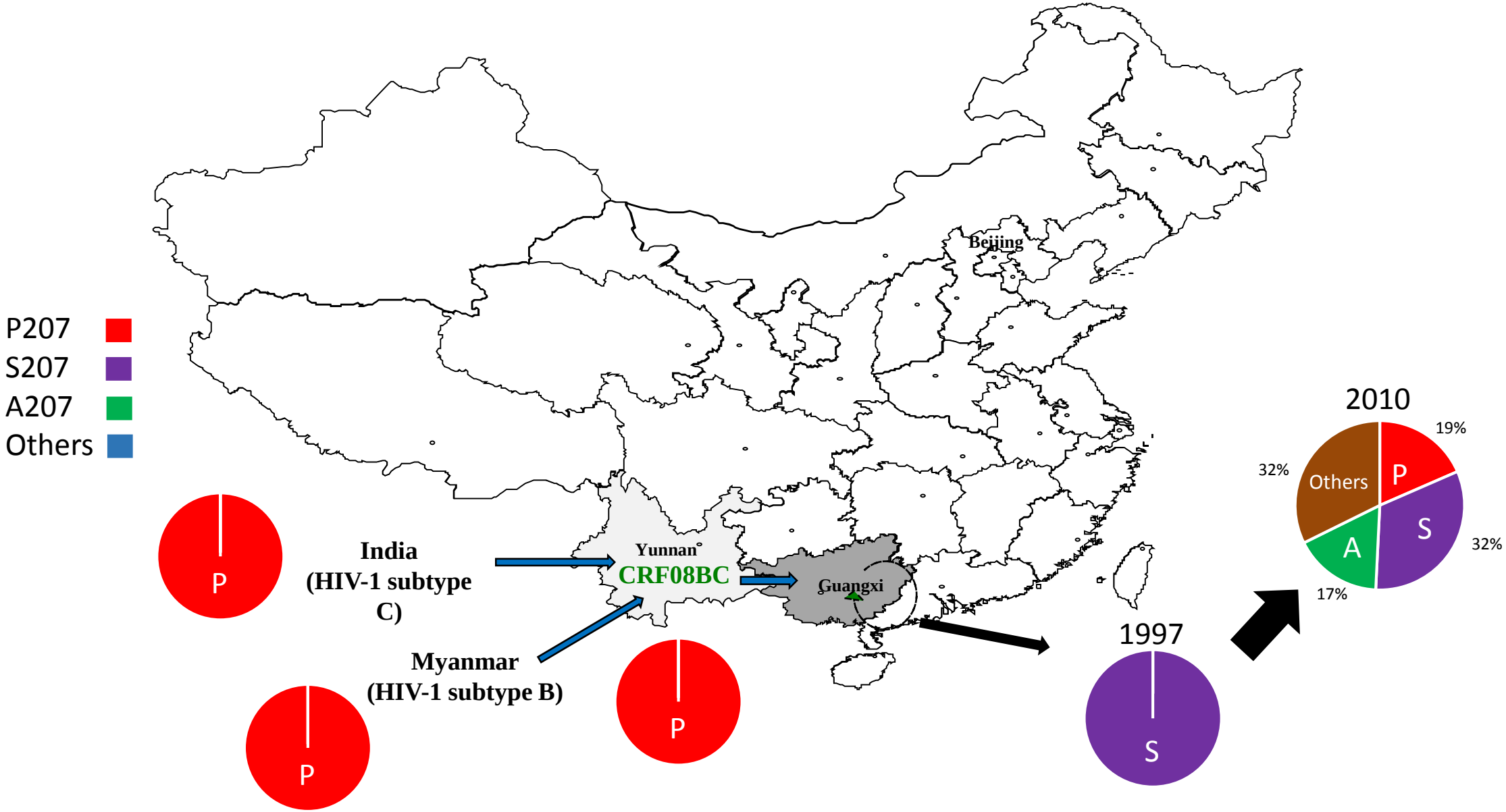
P207
S207
A207
Others
Beijing
Yunnan
CRF08BC
Guangxi
India
(HIV-1 subtype C)
Myanmar
(HIV-1 subtype B)
P
P
P
1997
S
2010
19%
32%
32%
17%
Others
P
S
A

Fig. S4

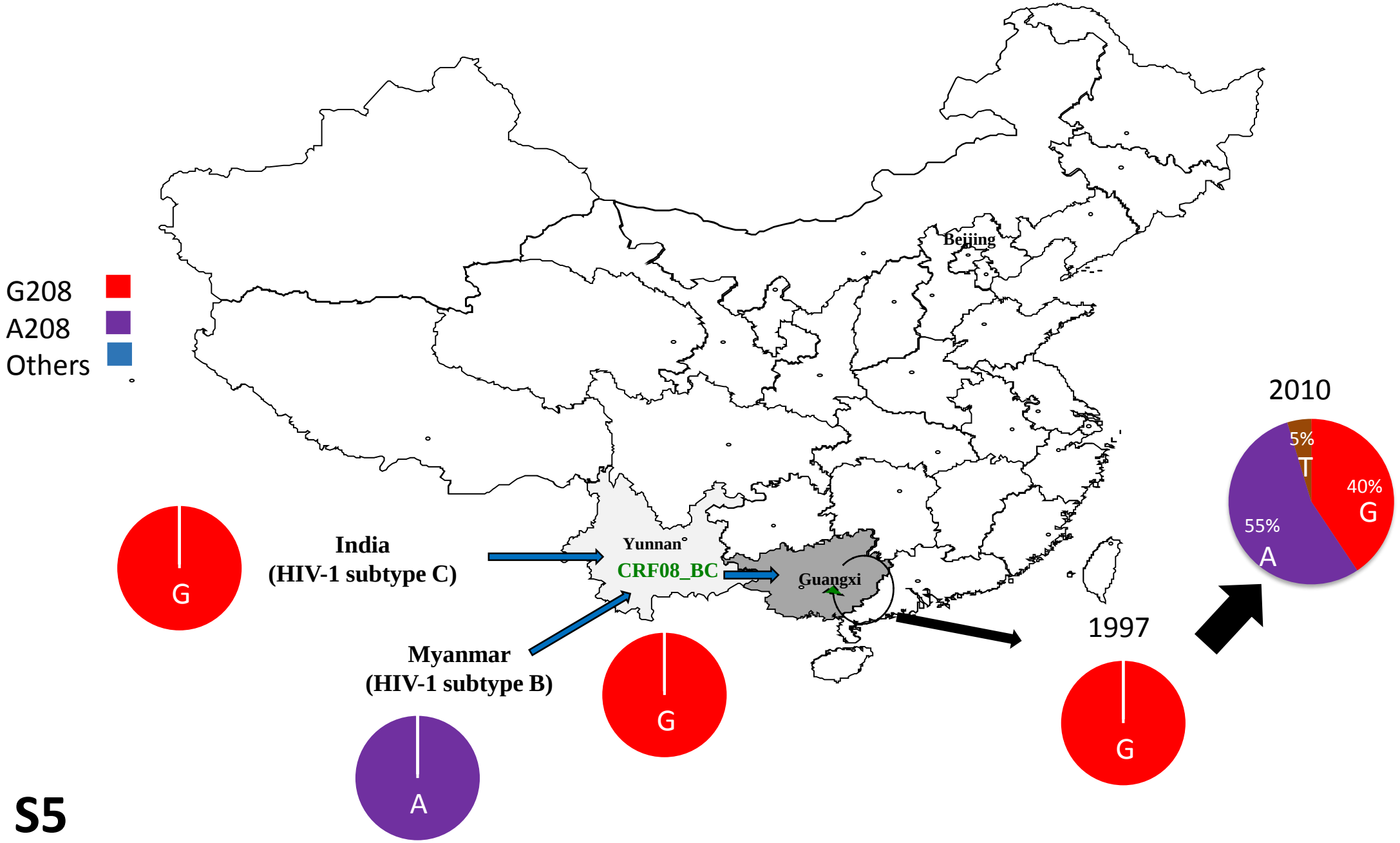
G208
A208
Others
Beijing
Yunnan
Guangxi
India
(HIV-1 subtype C)
CRF08_BC
Myanmar
(HIV-1 subtype B)
G
A
G
1997
G
2010
5%
T
40%
G
55%
A

Fig. S5

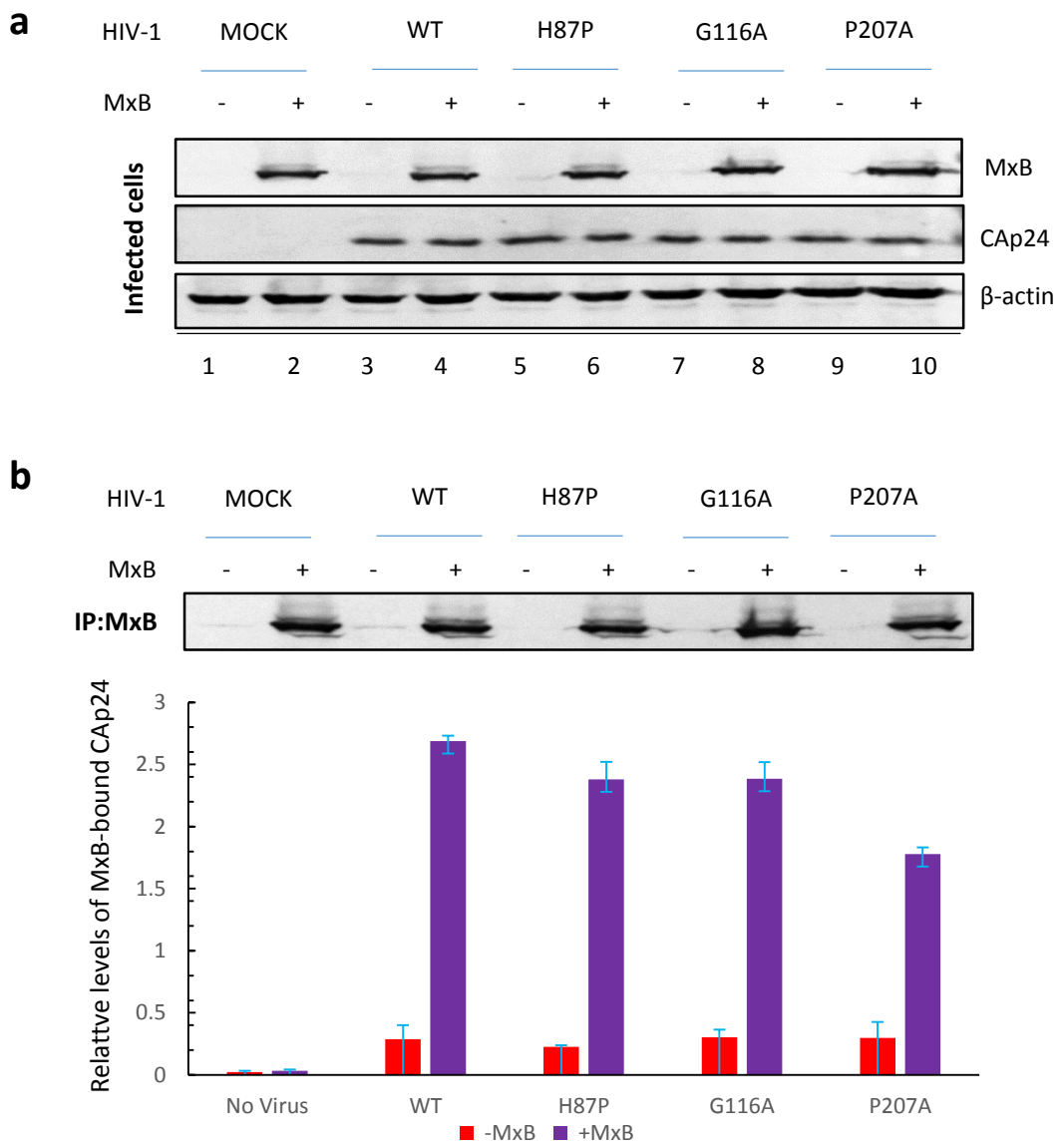
a
HIV-1
MOCK
WT
H87P
G116A
P207A
MxB
- + - + - + - + - +
Infected cells
MxB
CAp24
β-actin
1 2 3 4 5 6 7 8 9 10
b
HIV-1
MOCK
WT
H87P
G116A
P207A
MxB
- + - + - + - + - +
IP:MxB
Relattve levels of MxB-bound CAp24
3
2.5
2
1.5
1
0.5
0
No Virus
WT
H87P
G116A
P207A
-MxB
+MxB

Fig. S6

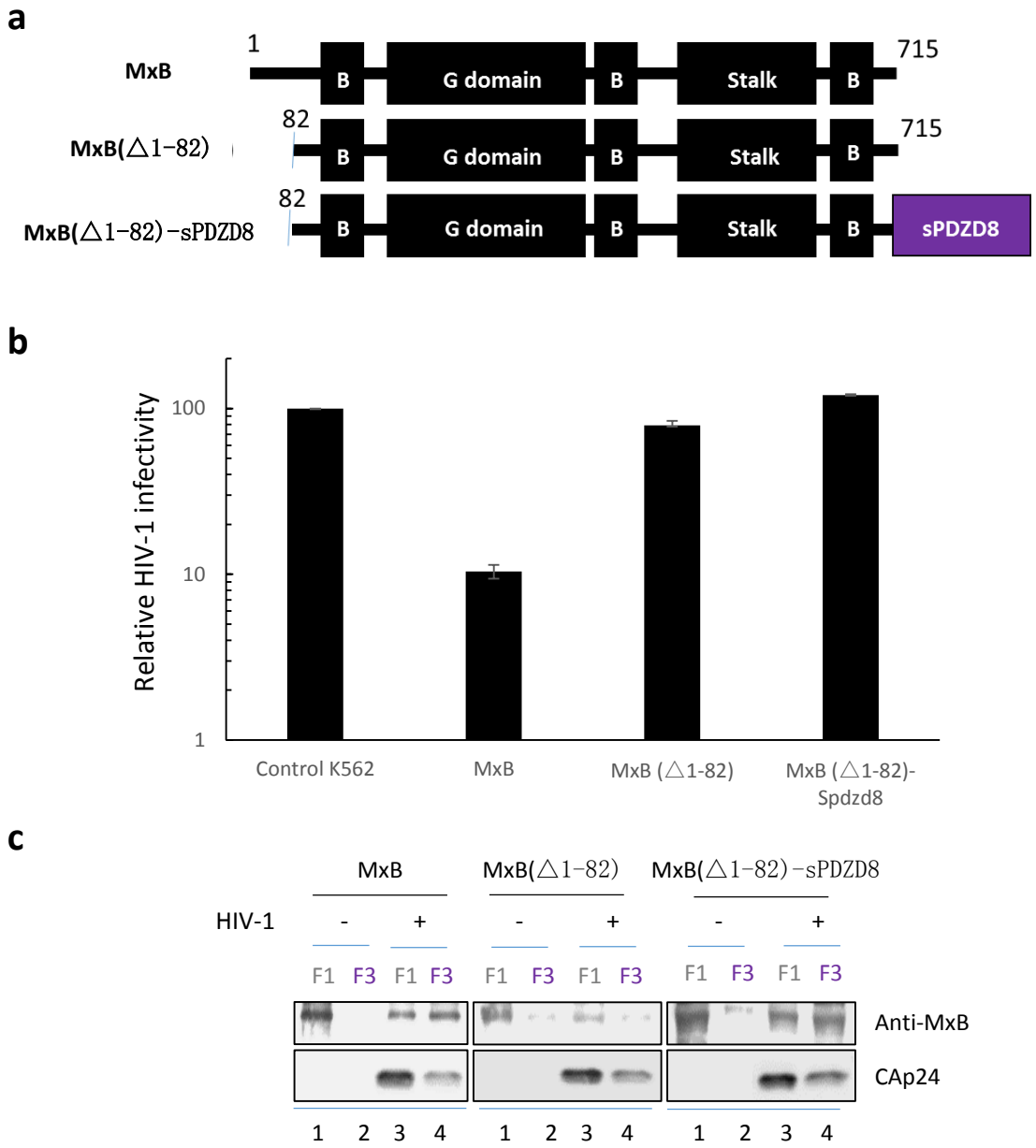
a
MxB
1
715
B
G domain
B
Stalk
B
MxB(△1-82)
82
715
MxB(△1-82)-sPDZD8
82
sPDZD8
b
Relative HIV-1 infectivity
100
10
1
Control K562
MxB
MxB (△1-82)
MxB (△1-82)-Spdzd8
c
MxB
MxB(△1-82)
MxB(△1-82)-sPDZD8
HIV-1
-
+
F1
F3
Anti-MxB
CAp24
1
2
3
4

Fig. S7

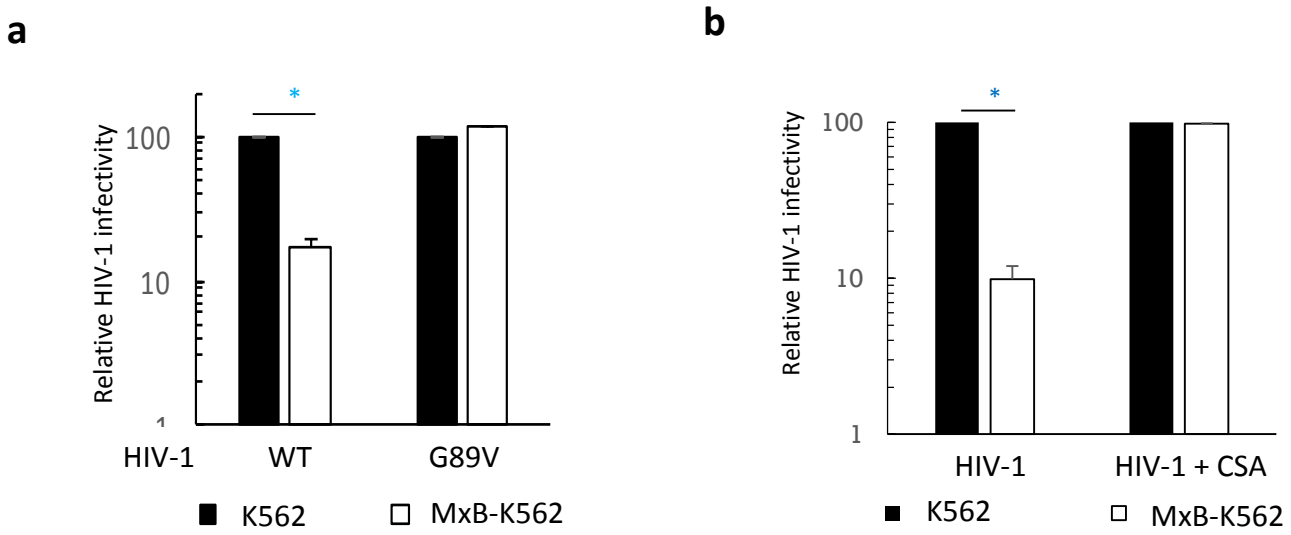
a
*
Relative HIV-1 infectivity
100
10
1
HIV-1
WT
G89V
K562
MxB-K562
b
*
Relative HIV-1 infectivity
100
10
1
HIV-1
HIV-1 + CSA
K562
MxB-K562

Fig. S8

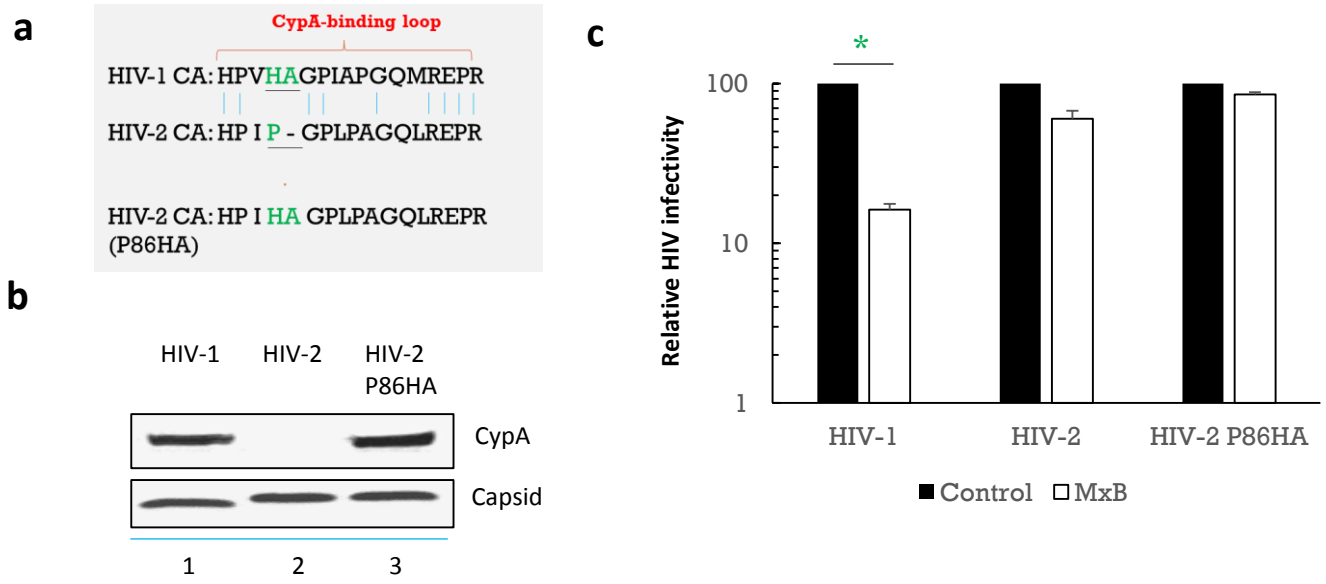
a
CypA-binding loop
HIV-1 CA: HPVHAGPIAPGQMREPR
HIV-2 CA: HP I P - GPLPAGQLREPR
HIV-2 CA: HP I HA GPLPAGQLREPR
(P86HA)
b
HIV-1
HIV-2
HIV-2
P86HA
CypA
Capsid
1
2
3
c
*
100
10
1
Relative HIV infectivity
HIV-1
HIV-2
HIV-2 P86HA
Control
MxB

Fig. S9

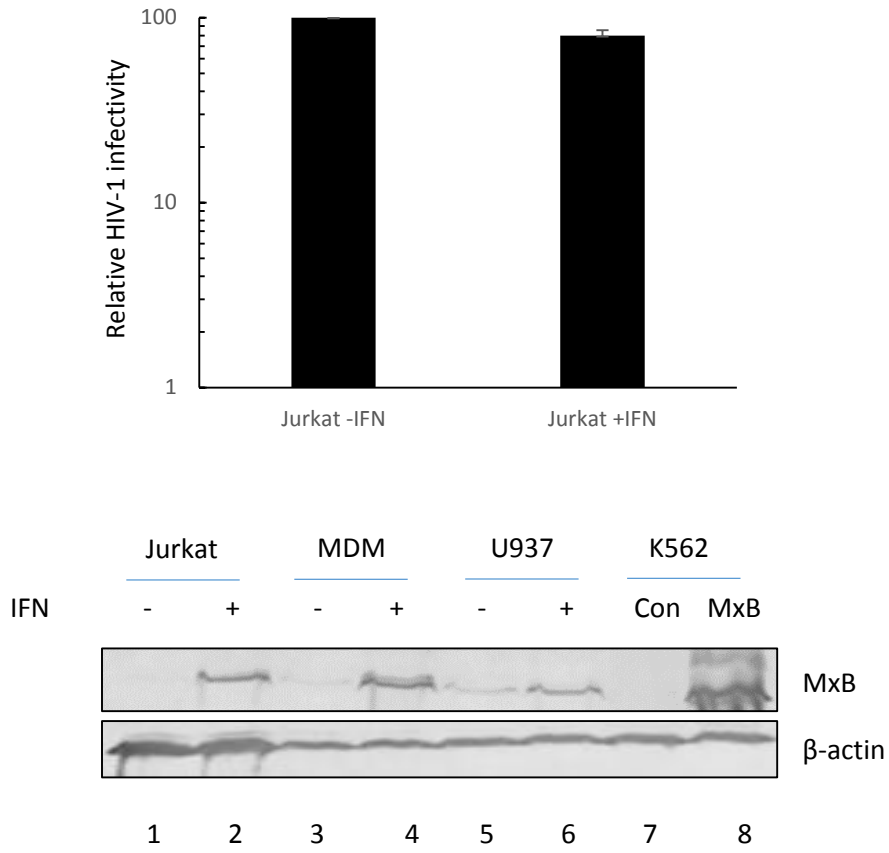
100
10
1
Relative HIV-1 infectivity
Jurkat -IFN
Jurkat +IFN
Jurkat
MDM
U937
K562
IFN
-
+
-
+
-
+
Con
MxB
MxB
β-actin
1
2
3
4
5
6
7
8

Fig. S10

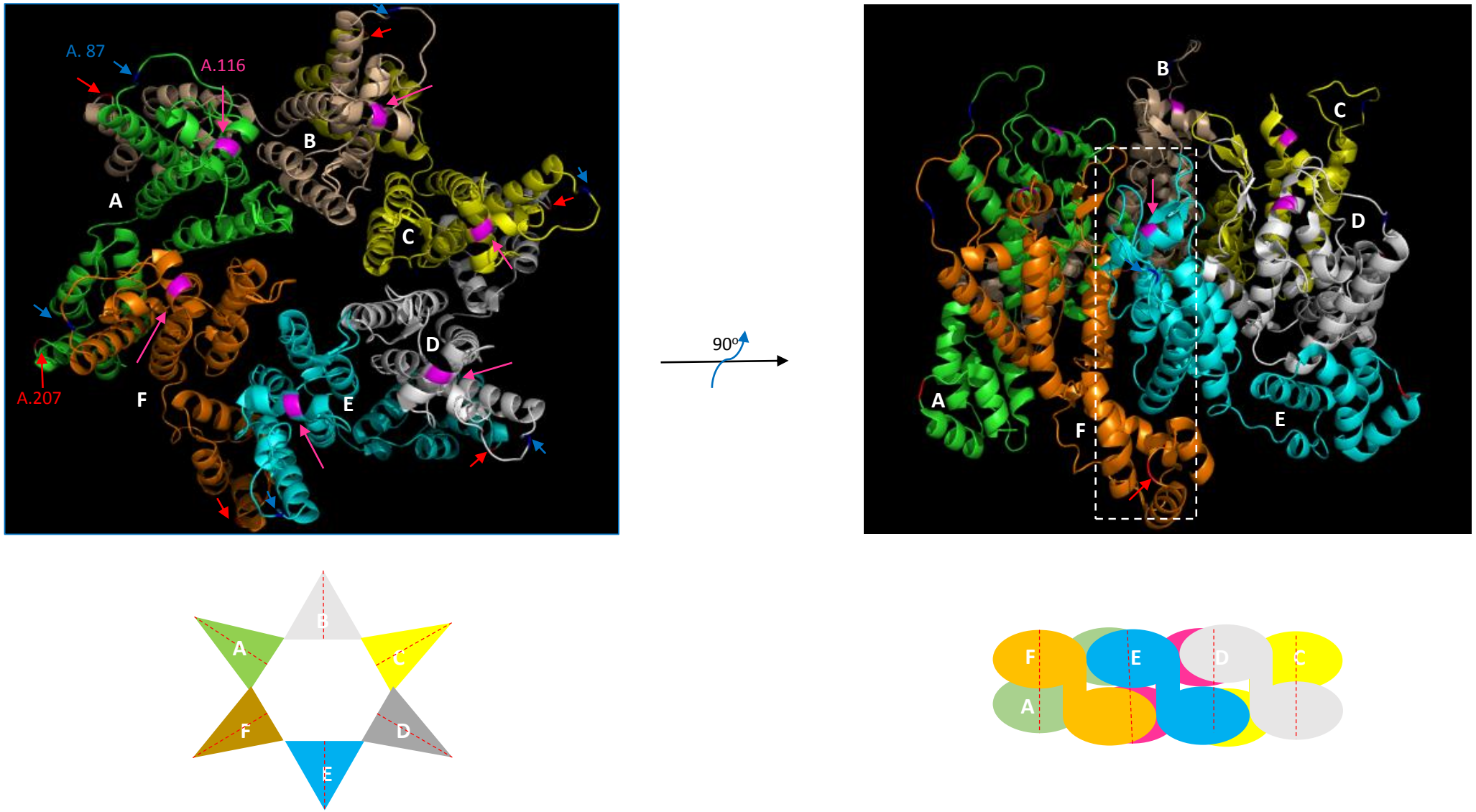

Fig. S11